UNIVERSITY OF CALIFORNIA SAN DIEGO

MG-132 is a broad-spectrum cysteine and aspartyl protease inhibitor

A Thesis submitted in partial satisfaction of the requirements
for the degree Master of Science

in

Biology

by

Dustin Pwee

Committee in charge:

Professor Anthony O'Donoghue, Chair
Professor Brenda Bloodgood, Co-Chair
Professor Sonya Neal

2022

The Thesis of Dustin Pwee is approved, and it is acceptable in quality and form for publication on microfilm and electronically.

University of California San Diego

2022

TABLE OF CONTENTS

.

LIST OF FIGURES

LIST OF TABLES

LIST OF ABBREVIATIONS

DMSO	Dimethyl sulfoxide
K-AMC	Lys-7-amino-4-methylcoumarin
IQ5	Mca-GKPILFFRLK(DNP)dR -NH2
AAPV-AMC	MeOSuc-Ala-Ala-Pro-Val-AMC
MSP-MS	Multiplex Substrate Profiling by Mass Spectrometry
TTSP	Type II transmembrane serine proteases
TMPRSS2	Transmembrane serine protease 2
Kbt	Ketobenzothiazole
MERS-CoV	Middle East Respiratory Syndrome Coronavirus
CatL	Cathepsin L
CatB	Cathepsin B
HGF	Hepatocyte growth factor
Mpro	Main protease
PLpro	Papain-like protease

ACKNOWLEDGEMENTS

I would like to express my sincere gratitude to my advisor, Dr. Anthony O'Donoghue, for his invaluable mentorship and constant support. He patiently guided me through multiple projects and provided me with a strong foundation in scientific research. I would also like to thank the members of the O'Donoghue Lab and Caffrey Lab for their help and support. Additionally, I wish to acknowledge my committee members Dr. Brenda Bloodgood and Dr. Sonya Neal for their support. Finally, I am grateful for my family and friends for their encouragement and confidence in me.

Chapter 3, in part, is a reprint of the material as it appears in A novel class of TMPRSS2 inhibitors potently block SARS-CoV-2 and MERS-CoV viral entry and protect human epithelial lung cells. Mahoney, Matthew, Damalanka, Vishnu C., Tartell, Michael A., Chung, Dong H., Lourenço, André L., Pwee, Dustin, Bridwell, Anne E.M., Hoffmann, Markus, Voss, Jorine, Karmakar, Partha, Klingler, Andrea M., Thompson, Cassandra E., Lee, Melody, Klampfer, Lidija, Stallings, Christina L., Rothenberg, Marc E., Whelan, Sean P.J., O'Donoghue, Anthony J., Craik, Charles S., Janetka, James W., Proceedings of the National Academy of Sciences, 2021. The thesis author was a co-author of this paper.

Chapter 4, in part, is a reprint of the material as it appears in Potent Anti-SARS-CoV-2 Activity by the Natural Product Gallinamide A and Analogues via Inhibition of Cathepsin L. Ashhurst, Anneliese S., Tang, Arthur H., Fajtová, Pavla, Yoon, Michael C., Aggarwal, Anupriya, Bedding, Max J., Stoye, Alexander, Pwee, Dustin, Drelich, Aleksandra, Li, Linfeng, Meek, Thomas D., McKerrow, James H., Tseng, Chien-Te, Larance, Mark, Turville, Stuart, Gerwick, William H., O'Donoghue, Anthony J., Payne, Richard J., Journal of Medicinal Chemistry, 2022. The thesis author was a co-author of this paper.

VITA

2021 Bachelor of Science in Human Biology, University of California San Diego

2022 Master of Science in Biology, University of California San Diego

PUBLICATIONS

Ashhurst AS, Tang AH, Fajtová P, et al. Potent Anti-SARS-CoV-2 Activity by the Natural Product Gallinamide A and Analogues via Inhibition of Cathepsin L. *J Med Chem*. 2022;65(4):2956-2970. doi:10.1021/acs.jmedchem.1c01494.

Mahoney M, Damalanka VC, Tartell MA, et al. A novel class of TMPRSS2 inhibitors potently block SARS-CoV-2 and MERS-CoV viral entry and protect human epithelial lung cells. *Proc Natl Acad Sci U S A*. 2021;118(43):e2108728118. doi:10.1073/pnas.2108728118.

ABSTRACT OF THE THESIS

MG-132 is a broad-spectrum cysteine and aspartyl protease inhibitor

by

Dustin Pwee

Master of Science in Biology

University of California San Diego, 2022

Professor Anthony O'Donoghue, Chair
Professor Brenda Bloodgood, Co-Chair

MG-132 is a tripeptide-aldehyde (Cbz-leu-leu-leucinal) and is extensively used in cellular studies to understand the role of the proteasome in cells as it is a potent inhibitor of the human proteasome. Early articles of MG-132 revealed its ability to inhibit cysteine cathepsins and calpains (1) and advised the community that controls such as a cysteine protease inhibitor also be used distinguish between cellular function of the proteasome and that of cysteine proteases. Many papers in the last 25 years have made conclusions about the proteasome based on

phenotypic changes that have occurred following treatment with MG-132 but without a control compound.

We previously determined that MG-132 is not only a potent inhibitor of cathepsin B and cathepsin L, but also potently inhibits the aspartyl proteases, cathepsin D and E. We then assayed HeLa and A549 lysates for protease activity at pH 3.5 and 5.5 with MG-132 and observed complete inhibition with 10 μM of MG-132 while other proteasome inhibitors such as marizomib, bortezomib and carfilzomib did not significantly inhibit this enzyme activity. In dose response assays with A549 lysate, we determined that the IC50 value for MG-132 at pH 3.5 and pH 5.5 was 5.0 nM and 8.7 nM, respectively. In summary, MG-132 is a potent inhibitor of aspartyl protease and cysteine protease within the concentration range that is used in cellular studies. Therefore, the phenotypic and biochemical changes that occur upon treatment of cells with this inhibitor are unlikely to be solely due to inhibition of the proteasome.

CHAPTER 1

The proteasome is a multiunit proteolytic complex involved in the ubiquitin-proteasome pathway in eukaryotic cells. It is involved with the regulation of multiple different cellular mechanisms and physiological processes including cell proliferation and gene expression. Many diseases have been attributed to upregulation or dysfunction of the ubiquitin-proteosome complex (1). Proteosome inhibitors are useful tools for understanding the role of the proteosome and were utilized to demonstrate that the proteosome hydrolyzes not only a majority of transient but also long-lasting proteins in mammalian cells. Proteosome inhibitors have also been studied for their therapeutic potential for cancer and other diseases (2). Multiple myeloma is a cancer of the plasma cells and inhibits blood cell formation and leads to systemic disease. Bortezomib and Carfilzomib are both FDA-approved proteasome inhibitors for multiple myeloma treatment. These inhibitors are also being studied for other cancers and inflammatory diseases, as well as immunosuppression.

Another popular proteasome inhibitor is MG-132, which decreases cell growth and induces apoptosis in mammalian cells. MG-132 has been utilized as a popular proteasome inhibitor because it is potent, affordable, and reversible. Synthesized by Alfred L. Goldberg and colleagues, MG132 was one of the first peptide aldehyde proteasome inhibitors to be developed. It was designed based on the substrate specificity of the proteasome's chymotrypsin-like active site (1). Peptide aldehydes are also potent inhibitors of cysteine and serine proteases, including cathepsin and calpain proteases. Because MG132 can inhibit calpains and cathepsins in addition to proteasomes, it is imperative to perform control experiments when using MG132 to confirm that the observed effects are due to proteasome inhibition and not inhibition of other proteases. Protease involvement can also be confirmed or ruled out with more specific proteasome

inhibitors, such as lactacystin and epoxomicin (1), but that have not been used as often as MG-132 for cellular studies. Although there are other proteasome inhibitors available, MG132 is regarded as the inhibitor of choice for studying the role of the proteasome in cells. However, control compounds, such as the cysteine protease inhibitor, E-64, must be included for proper data analysis and interpretation.

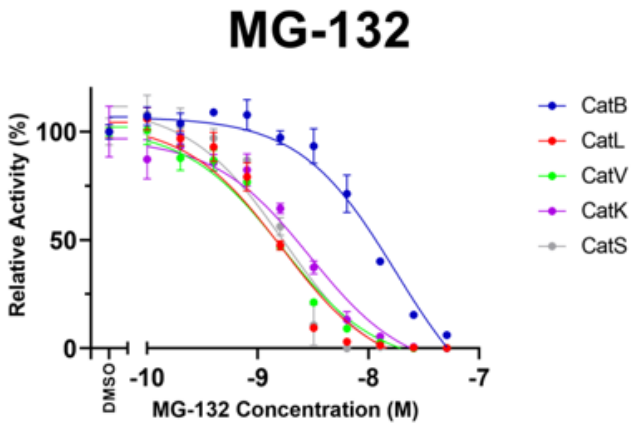

	CatB	CatL	CatV	CatK	CatS
IC50 (nM)	17.64	1.652	1.634	2.953	1.742

Figure 1.1: Cysteine protease dose response curves at pH 5.5.

We previously determined that MG-132 is not only a potent inhibitor of cathepsin B and cathepsin L, but also potently inhibits the aspartyl proteases, cathepsin D and E (Figure 1.1). Therefore, the enzyme inactivates at least 4 major proteases within the endo-lysosomal degradation system. To evaluate its effect in cells, we generated lysates of A549 and HeLa cells and assayed for aspartyl protease activity at pH 3.5 and for cysteine protease activity at pH 5.5 in the absence and presence of MG-132. Using pepstatin as a control inhibitor for pH 3.5 and E64 for pH 5.5, we observed complete inhibition of aspartyl and cysteine protease activity with 10 µM of MG-132 at pH 3.5 and pH 5.5, respectively, while other proteasome inhibitors tested including marizomib, bortezomib and carfilzomib did not significantly inhibit this enzyme

activity. We performed a dose response assay at pH 3.5 with A549 lysate and showed that the IC50 for MG-132 and pepstatin was 5.0 nM and 0.48 nM, respectively. At pH 5.5 with the lysate, the IC50 of MG-132 and E64 was 8.7 nM and 6.0 nM, respectively. We show that MG-132 is an inhibitor of aspartyl proteases and cysteine proteases and that it retains its potency within the concentration range that is used in cellular studies.

Materials and Methods

1. Cell culture, lysate preparation and protein quantification.

HeLa cells were cultured in Gibco Dulbecco's Modified Eagle Medium (DMEM) containing 10% FBS and 1% penicillin–streptomycin in T175 flasks. After 75% confluence was confirmed under microscope, the cells were washed with 10 mL of PBS to remove media. After PBS removal, the cells were incubated in 4 mL of trypsin/EDTA for 3 minutes to detach the cells from the flask. Once successful cell detachment was confirmed, 10 ml of DMEM was added and mixed. The cells were then transferred into a 50 mL Falcon conical tube and centrifuged at 2,000 rpm for 5 minutes at 25 ℃. The supernatant was discarded and 10 mL of DMEM was added to the tube and mixed with the pellet. To continue passaging the cells, 200 µL of cells were transferred into a new T175 flask with 30 mL of DMEM and stored in an incubator. The remaining cells were washed twice with 10 mL and 5 mL of PBS and then transferred to a 15 mL Falcon tube and centrifuged for a second cycle. After supernatant was removed, 1 mL of PBS was mixed with the pellet and transferred to a sterile 1.5 mL Eppendorf tube. The cells were centrifuged at 2,000 rpm for 5 minutes at 4 ℃. The supernatant was removed, and the pestle was frozen in ethanol and dry ice and stored at -80 ℃. A549 cells were obtained from the Akuthota Lab at UCSD School of Medicine. Protein extracts were generated from HeLa cells and A549

cells with 100 µL of ice-cold PBS and three freeze-thaw cycles at -80°C and 37°C, respectively. During thawing, samples were manually disrupted with mortar and pestle for 60 seconds followed by 15 seconds of mixture using vortex. A sonication probe was then inserted into the sample vial on ice and set to an amplitude of 20%. Sonication was applied for 20 cycles of one second activation with five second rest in between each cycle. Sonicated samples were centrifuged at 14,000 rpm for one minute. The supernatant was extracted and aliquoted for storage at -80°C. Protein concentration was determined with reference to bovine serum albumin standards in a BCA Assay kit from Thermo Scientific™.

2. Cell lysate inhibitor assays.

HeLa and A549 cell lysates were assayed at a final concentration of 30 µg/mL with either 50 µM Z-FR-AMC in 50 mM Na-Ac pH 5.5, 1 mM EDTA, 5 mM DTT or 13.5 µM Mca-GKPILFFRLK(DNP)dR-NH2 (IQ5) in citrate phosphate pH 3.5. 20 µM of MG132, pepstatin, E64, carfilzomib, bortezomib, and marizomib was pre-incubated for 30 minutes with HeLa and A549 cell lysates at room temperature prior to the addition of substrate. The final concentration of inhibitor in the assay was 10 µM. Assays were performed with a total volume of 30 µL in triplicate wells of black 384-well plates. Fluorescence was measured in 44 s intervals for 120 minutes at an excitation of 360 nm and emission of 460 nm on a Biotek HTX plate reader. DMSO was used as a vehicle control. For dose-response studies, 30 µg/mL HeLa and A549 cell lysate were preincubated for 30 minutes at 25 °C with 27,000 to 0.46 nM of inhibitor in 50 mM Na-Ac pH 5.5, 1 mM EDTA, 5 mM DTT or citrate phosphate pH 3.5. Proteolytic activity was detected at pH 5.5 and pH 3.5 with 50 µM Z-FR-AMC or 13.5 µM IQ5, respectively, in triplicate wells. The inhibitor assays were performed on duplicate plates with the IC50 calculated from dose-response curves in GraphPad Prism.

Results

We found that at pH 5.5, MG-132 and E64 potently inhibited proteolytic activity in both the A549 and HeLa lysates when Z-FR-AMC was used as the substrates, while the other inhibitors showed no inhibition (Figure 1.2). Since cysteine proteases are optimally activated at pH 5.5 and E64 is also a broad-spectrum cysteine protease inhibitor, we concluded that the proteolytic activity observed can be attributed to cysteine proteases.

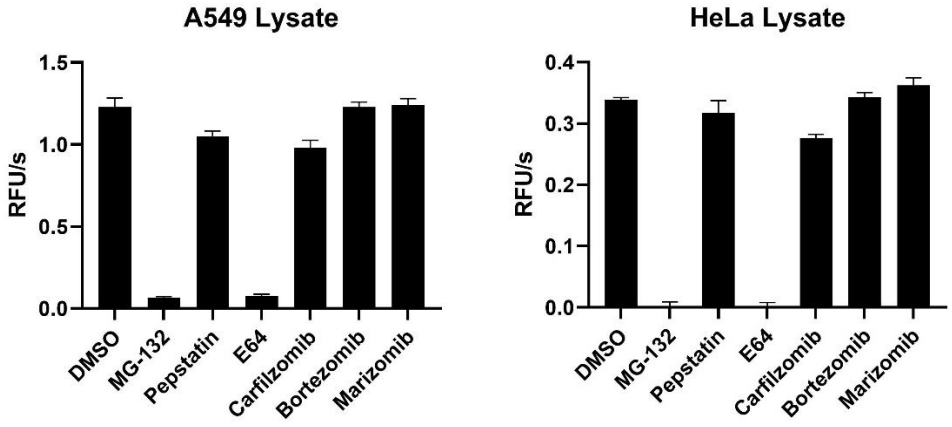

Figure 1.2: Inhibitor panel at pH 5.5. MG132 inhibits cysteine proteases at pH 5.5.

After we confirmed potent inhibition from both MG132 and E64 at pH 5.5, we quantified the amount of inhibition in a dose response. A549 and HeLa lysates were diluted to 30 µg/mL in assay buffer and incubated with 27000 to 0.46 nM of MG132 and E64. After 30 minutes of preincubation, we initiated the reaction with the addition of Z-FR-AMC at 50 µM. The IC50 of MG132 and E64 with A549 lysate was determined to be 8.67 nM and 6.0 nM respectively (Figure 1.3). Using the HeLa lysate, the IC50 of MG132 and E64 were 7.7 nM and 3.3 nM, respectively (Figure 1.3). Both compounds exhibit potent inhibitory effects regardless of cell

lysate in the low nanomolar range. Similar potency from both inhibitors in each cell line indicates that the results observed are not specific for a cell line or cell type.

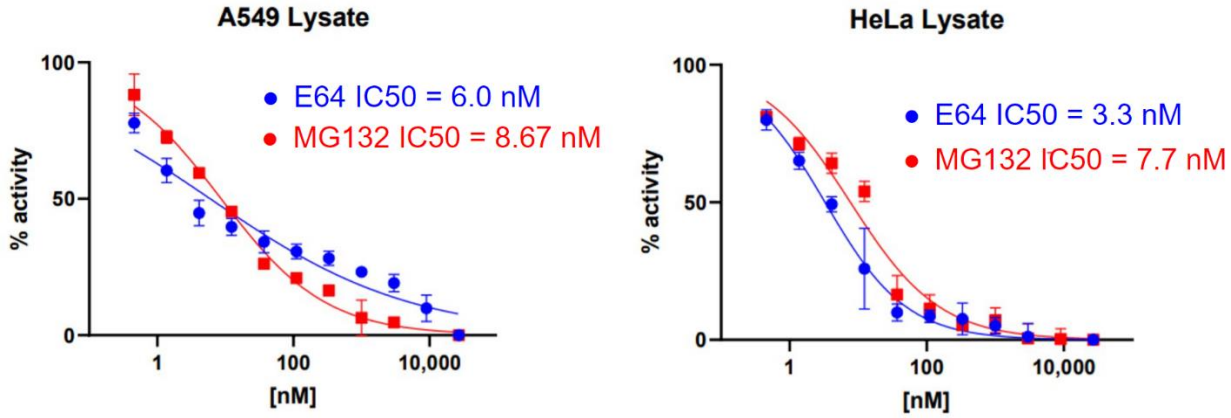

Figure 1.3: Dose response curves at pH 5.5.

We performed similar experiments at a lower pH of 3.5 to study the aspartyl proteases. The same inhibitor panel was incubated at 10 µM with both cell lines at 30 µg/mL in citrate phosphate pH 3.5 for 30 minutes. Aspartyl protease activity was quantified using a final concentration of 13.5 µM of the internally quenched fluorogenic substrate Mca-GKPILFFRLK(DNP)dR -NH2 (IQ5) where cleavage occurs between the two phenylalanine residues.

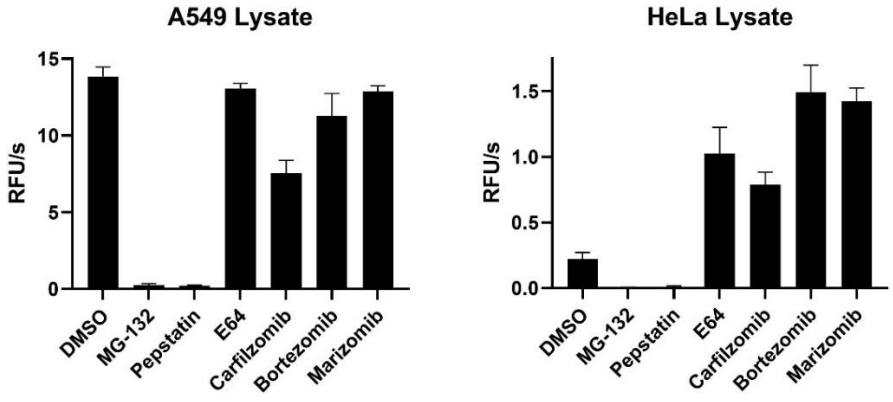

Figure 1.4: Inhibitor panel at pH 3.5. MG132 inhibits aspartyl proteases at pH 3.5.

When compared to a control reaction (DMSO), MG-132 and pepstatin potently inhibited proteolytic activity in both the A549 and HeLa lysates, while the other inhibitors showed insignificant inhibition (Figure 1.4). Aspartyl proteases are most optimal at pH 3.5 and pepstatin is a common aspartyl protease inhibitor, indicating that this protease family is responsible for the proteolytic activity observed here. Carfilzomib showed moderate inhibition, so it was included in our dose response assay. We performed a standard dose response assay and determined the IC50 of MG132 to be 5.04 nM and the IC50 of pepstatin to be 0.487 nM (Figure 1.4). Carfilzomib did not show inhibition at the concentration range tested. MG132 and pepstatin are potent inhibitors at pH 3.5, which is most likely due to aspartyl protease inhibition.

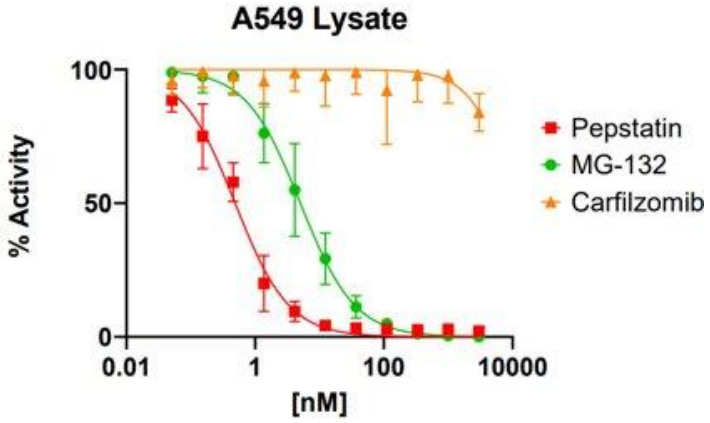

Figure 1.5: Dose response curve at pH 3.5.

While MG-132 has been popularly used as a proteasome inhibitor, it is important to consider whether the phenotypic effects observed in cell culture experiments is solely due to proteasome inhibition. We show that MG-132 is a potent, multifunctional inhibitor of both cysteine and aspartyl proteases and must be accounted for with control experiments. Future studies will involve cathepsin and proteasome dose-response assays.

Discussion

MG-132 is still the most used proteasome inhibitor for human cell culture studies. The recommended concentration range for MG-132 in these studies is 5 to 50 μM for up to 20 hours. MG-132 inhibits lysosomal cysteine proteases in HeLa and A549 cell extracts at pH 5.5 with similar potency to cysteine protease inhibitor E64. The target enzymes are likely to be cathepsin B, L, V and S as they all cleave Z-FR-AMC and are sensitive to E-64. MG-132 is also a potent endosomal and lysosomal aspartyl protease and inactivates most proteases in the endo-lysosomal pathway, including cathepsin D and E. While MG-132 is effective as a proteasome inhibitor, there are more specific proteasome inhibitors that can be used to study phenotypic changes from proteasome inhibition in cell studies, such as Bortezomib, Carfilzomib, and Marizomib. Cellular changes observed in cell treatment with MG-132 are unlikely to be solely due to proteasome inhibition.

CHAPTER 2

Asthma is a chronic respiratory disease associated with significant deterioration of patient quality of life and high healthcare costs. While a sizable proportion of asthma cases are moderated with inhaled corticosteroid treatments, disease heterogeneity has caused many patients to remain with high symptom scores and exacerbations. A novel approach of asthma treatment methods has been focused on individualized asthma endotypes and the immunological systems associated. Currently, there are two main subtypes of asthma dependent on the associated inflammatory pathway. The TH2-high endotype is characterized by significant activation of the allergic pathways and elevated levels of eosinophilia in the lung tissue (3). Conversely, the TH2-low endotype can be characterized by the lack of allergic activation and associated neutrophilic inflammation (3). As the heterogeneity of asthma has become well recognized in recent years, the phenotyping and endotyping of asthma has taken an increasingly central position in asthma investigation from both a mechanistic and therapeutic perspective. With the emergence of endotype-specific treatments, it is important to be able to accurately differentiate asthma endotypes with biomarkers.

Sputum cytology for eosinophils and neutrophils can be used as a research tool for asthma endotype identification. However, proper equipment and technical expertise would be required for sample processing and analysis, which may not be available in a clinical setting. Therefore, alternative methods of asthma endotype identification via sputum analysis must be explored. There is an abundance in proteases in both neutrophils and eosinophils, and many of these enzymes are involved with the white blood cell's immunological mechanism of action. By determining active proteases that are exclusive in either eosinophils or neutrophils, we can identify a new biomarker for asthma endotype.

Materials and Methods

1. Cell lysate preparation and protein quantification.

Isolated blood eosinophils and neutrophils from four healthy donors were obtained from the Akuthota Lab at UC San Diego School of Medicine. Lysates were prepared in 100 µL ice-cold PBS with three freeze-thaw cycles at -80°C and 37°C, respectively. During thawing, samples were manually disrupted with mortar and pestle for 60 seconds followed by 15 seconds of mixture using vortex. A sonication probe was then inserted into the sample vial for 20 cycles of 1 second activation and 5 second rest in between each cycle followed by centrifugation for 5 minutes. The protein supernatant was extracted and aliquoted for storage at -80°C. Protein concentration was determined with reference to bovine serum albumin standards in a BCA Assay kit from Thermo Scientific™ .

2. Identification of peptide cleavage sites by multiplex substrate profiling-mass spectrometry.

Eosinophil and neutrophil lysates were incubated at 2 µg/mL with a substrate library of 228 tetra decapeptides in DPBS containing 0.01% Tween. The peptides were mixed at equal molar concentration and diluted to 500 nM in assay buffer. Aliquots were removed from both lysates at different time points (15, 60, and 240 minutes) and quenched with 8M guanidinium hydrochloride. All assays were completed in quadruplicate reaction tubes. Aliquots were desalted using C18 spin columns and analyzed by nano-LC-MS/MS peptide sequencing using an LTQ Orbitrap mass spectrometer. Peptide cleavage from the substrate library was detected and quantified using PEAKS bioinformatics software. For each cleavage product formed, the turnover rate (kcat/Km) is calculated from progress curves using the first-order kinetic formula $Y=(plateau-Y0) \times (1-exp(-t \times kcat/Km \times [E0])) + Y0$.

3. Cell extract fluorescence assays.

Blood eosinophil and neutrophil extracts from four healthy donors were assayed in DPBS containing 0.01%. The reaction was initiated with the addition of 50 μM of fluorogenic substrate and fluorescence was measured at 360/460 nm (ex/em) using a Biotek HTX plate reader. All assays were performed in biological quadruplicates on black 384-well plates with a final volume of 30 μL.

Results

To evaluate cell-type specific proteolytic signatures, we incubated eosinophil and neutrophil protein extracts with the MSP-MS reporter substrates. Each substrate in the library contains 13 cleavable peptide bonds and cleavage of any of the 2,964 peptide bonds were detected. We determined that 27 of the possible 2,964 peptide bonds were cleaved (Figure 2.1). We identified one peptide with the sequence K^SHTNDLPLISVMR to be efficiently cleaved between the K and S by eosinophil proteases. This indicates the presence of an aminopeptidase in the eosinophil lysate. We did not detect strong aminopeptidase in our previous studies with neutrophil extracts (4).

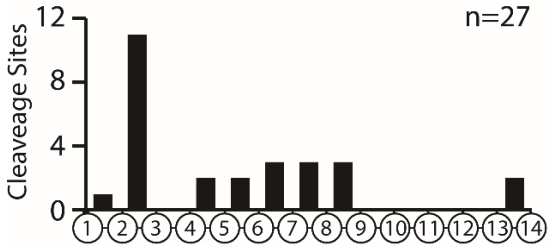

Figure 2.1: Distribution of cleavage sites withing the tetradecapeptide library.

To confirm the difference in aminopeptidase activity between eosinophils and neutrophils, we assayed protein extracts with fluorescent aminopeptidase substrate Lys-7-amino-4-methylcoumarin (K-AMC). This substrate mimics the K-SHTNDLPLISVMR substrate. We

determined that activity was 3-fold to 25-fold higher in eosinophils compared to neutrophils, which validates the results from the MSP-MS data (Figure 2.2). This also indicates a new reporter substrate that is selective for eosinophils. significantly more active than neutrophil proteases.

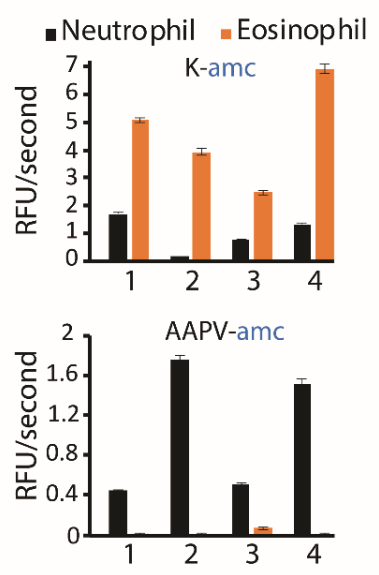

Figure 2.2: Fluorescent activity assay using aminopeptidase substrate (K-amc) and neutrophil elastase substrate (AAPV-AMC).

We generated a substrate signature of all the peptide products generated by eosinophil proteases from the MSP-MS assay and identified an overall preference for cleavage on the C-terminal side of Trp, Asp, Lys and His and on the N-terminal side of Pro, Tyr and Arg (Figure 2.3). Amino acids above x-axis are found with high frequency at sites surrounding the cleaved bond, while amino acids below the x-axis are never found in these positions. The cleavage site is indicated with an arrow. This substrate profile has little similarity to the neutrophil protease profile previously generated by our lab that revealed a preference for cleavage on the C-terminal side of Val (4).

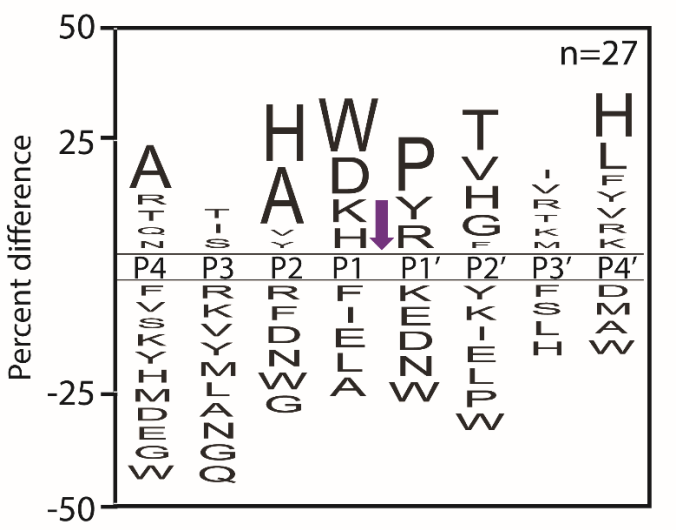

Figure 2.3: Protease substrate signature of eosinophil extracts.

Neutrophil protease activity is primarily attributed to neutrophil elastase, which is known to efficiently cleave fluorogenic substrate MeOSuc-Ala-Ala-Pro-Val-AMC (AAPV-AMC). We hypothesized that this activity is unique to neutrophils. We confirmed this after assaying both cell lysates with AAPV-AMC and saw strong activity in the neutrophil lysate but negligible activity in eosinophil proteases (Figure 2.2).

Discussion

These results from substrate profiling and selectivity of eosinophils and neutrophils indicate that the presence of exclusive proteases in either cell type. By identifying peptides that are selectively cleaved by either neutrophil or eosinophil proteases, we can synthesize fluorogenic reporter substrates to detect and quantify the individual proteases in neutrophil and eosinophil lysates using a standard microplate assay. Systematic development of selective substrates for quantifying proteolytic activity in cell extracts and sputum will allow for rapid and sensitive diagnostic testing of asthma endotype. Utilizing the MSP-MS assay to quantify

protease activity in neutrophil and eosinophil extracts, we will continue to characterize proteases in these samples and improve the substrates for selectivity and sensitivity.

CHAPTER 3

Severe Acute Respiratory Syndrome Coronavirus-2 (SARS-CoV-2) is the newly emerged, highly transmissible coronavirus responsible for the ongoing Coronavirus Disease 2019 (COVID-19) pandemic, which is associated with over 520 million cases and 6 million deaths worldwide as of May 12, 2022. While various vaccines have been approved by the FDA, there are still no clinically approved small molecule drugs available for the treatment of this disease except Remdesivir. Multiple therapeutic strategies have been proposed, including both viral and host proteins, but none have yet been fully validated for clinical application. One class of protein targets which have shown promising results are proteolytic enzymes including the viral proteases, Papain-Like Protease (PLpro) and the 3C-like or 'Main Protease' (3CL or MPro), and several host proteases involved in viral entry, replication, and effects on the immune system creating the life-threatening symptoms of COVID-19 infection. The latter include various members of the cathepsin family of cysteine proteases including cathepsin L, furin, and the serine proteases factor Xa, plasmin, elastase, tryptase, TMPRSS2 and TMPRSS4.

TMPRSS2 is a type II transmembrane serine protease (TTSP) that has been shown to be crucial for host-cell viral entry and spread of SARS-CoV-2, as well as SARS-CoV, Middle East Respiratory Syndrome Coronavirus (MERS-CoV) and influenza A viruses. Like SARS-CoV and MERS-CoV, SARS-CoV-2 cell entry involves binding of the viral spike protein to the host cell receptor Angiotensin Converting Enzyme-2. The spike protein requires proteolytic processing/priming by TMPRSS2 to mediate entry into lung cells, thus small molecule inhibitors of this target offer much promise as new therapeutics for COVID-19 and other coronavirus diseases. It has been demonstrated that the TMPRSS2-expressing lung epithelial Calu-3 cells are highly permissive to SARS-CoV-2 infection. The irreversible serine protease inhibitors Camostat

and Nafamostat are effective at preventing host cell entry and replication of SARS CoV-2 in Calu-3 cells through a TMPRSS2-dependent mechanism. We report on the discovery of a new class of substrate-based ketobenzothiazole (kbt) inhibitors of TMPRSS2 with potent antiviral activity against SARS-CoV-2 and which are significantly improved over Camostat and Nafamostat. Several compounds were found to be strong inhibitors of viral entry and replication. Newly developed compound MM3122 has excellent pharmacokinetics and safety in mice and is thus a promising new lead candidate drug for COVID-19 treatment.

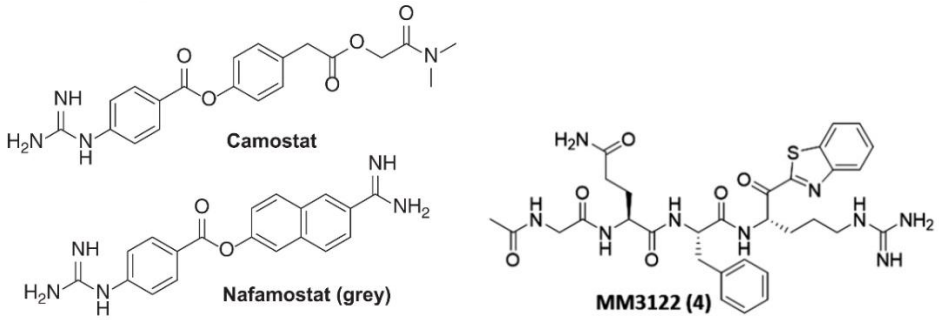

Figure 3.1: Structures of hit compound MM3122 and control inhibitors Camostat and Nafamostat.

Methods and Methods

1. Recombinant TMPRSS2 enzyme assays.

Active recombinant full-length TMPRSS2 was purchased from Cusabio Technology and assayed at a final concentration of 3 nM in 25 mM Tris-HCl, 150 mM NaCl, 5 mM Cacl2, 0.01% Triton X-100, pH 8.0, with fluorogenic substrate Boc-QAR-AMC to determine the Km. Boc-QAR-AMC was serially diluted in DMSO and then each diluent was further diluted in assay buffer so that the final substrate concentration in the assay ranged from 0.514 µM to 200 µM with a final DMSO concentration of 0.5%. The assay was performed in a total volume of 30 µL in triplicate wells of a black 384-well plate. Initial reaction velocity was measured in 35 second intervals for 7 minutes. Excitation of 360 nM and emission of 460 nM was recorded on a Biotek

HTX plate reader. For inhibitor studies, compounds were serially diluted 3-fold in DMSO and then preincubated with TMPRSS2 in assay buffer for 30 min at room temperature. The reaction was initiated following the addition of Boc-QAR-AMC and fluorescence was measured in 190 second intervals for 90 min. The final concentration of enzyme and substrate were 3 nM and 86.6 µM, respectively and the inhibitor concentrations ranged from 2 µM to 0.15 pM. Assays were performed in quadruplicate plates and IC50 was calculated from dose-response curves using Graphpad Prism.

Results

Several TTSPs, including TMPRSS2, not only play a role in infectious diseases, but also cancer progression and metastasis, which is thought to be primarily through its ability to activate hepatocyte growth factor (HGF), the sole ligand for MET receptor tyrosine kinase. This is accomplished via proteolytic processing of the inactive single-chain precursor pro-HGF to a two-chain active form. TMPRSS2 shares pro-HGF as a protein substrate with the other HGF-activating serine proteases, HGF-Activator, hepsin and matriptase. Like TMPRSS2, other TTSPs such as matriptase and hepsin have an established serine protease domain residing as the C-terminal domain of the protein that is anchored to the cell membrane by an N terminal type II signal peptide thereby presenting their enzymatic activity outside the cell. Our collaborators at Washington University School of Medicine had previously reported on the discovery and anticancer properties of peptidomimetic ketobenzothiazole inhibitors of HGFA, matriptase and hepsin named synthetic HGF Activation Inhibitors. Since TMPRSS2 has an overlapping endogenous substrate specificity profile with HGF-activating proteases, we hypothesized that these substrate-based HGF Activation Inhibitors would also inhibit TMPRSS2.

Using active recombinant full-length TMPRSS2 with serine protease substrate Boc-QAR-AMC, we calculated the Km to be 85.6 μM from Michaelis-Menten plots using GraphPad Prism (Figure 3.1). We used this substrate concentration to test 38 inhibitors for inhibition of TMPRSS2 proteolytic enzyme activity in a standard kinetic assay using Nafamostat and Camostat as controls.

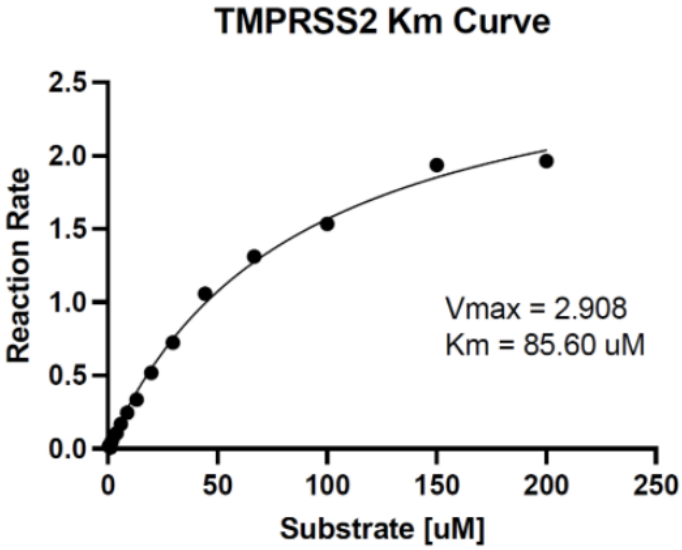

Figure 3.2: Km curve for Boc-QAR-AMC using full-length TMPRSS2.

We determined the compound IC50s over the period of one hour, following 30 minutes of compound incubation with enzyme. We determined that multiple compounds were more potent than Camostat and several were equipotent to Camostat (Table 3.2). Compounds 4-7 showed potent sub nanomolar IC50 values. It is important to note that Nafamostat is an irreversible inhibitor while the ketobenzothiazole class of inhibitors all reversibly inhibit. This makes direct comparison of IC50 values difficult as they have different mechanisms of inhibition.

Table 3.1: Structures and inhibition data of compounds with TMPRSS2.

Name/structure	TMPRSS2 IC50 (nM)
Camostat	1.5
Nafamostat	0.14
ZFH7116 (1)	74
VD2173 (2)	2.6
VD3173 (19)	19
VD4051 (21)	197
VD3152 (20)	ND
PK-1-102 (8)	9.4
ZFH6095 (9)	7.9
ZFH6101 (10)	29
ZFH6138 (11)	16
ZFH6201-1 (18)	54
ZFH7053 (3)	39
ZFH7063 (12)	3
PK-1-89 (13)	1.1
PK-1-18 (14)	39
PK-1-45A1 (15)	42
ZFH7064 (16)	6.3
ZFH7006 (17)	ND
MM3116 (7)	0.25
MM3144 (6)	0.31
MM3123 (4)	0.28
MM3122 (4)	0.34

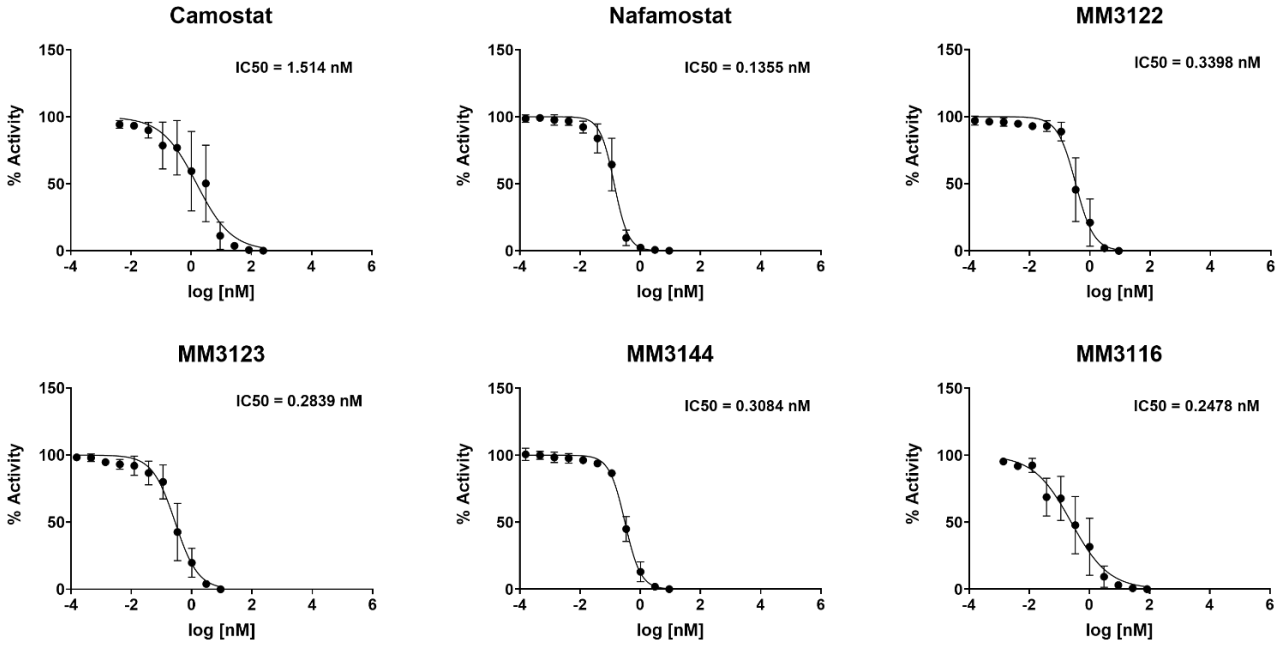

Figure 3.3: IC50 inhibition curves of full-length TMPRSS2/Boc-QAR-AMC.

Discussion

TMPRSS2 is shown to play a key role in host cell viral entry and replication of SARS-CoV-2. We hypothesized that previously reported peptidyl ketobenzothiazole inhibitors of HGFA, matriptase, and hepsin would also inhibit TMPRSS2. Using recombinant TMPRSS2, we determined that these compounds do in fact potently inhibit TMPRSS2 proteolytic activity. With TMPRSS2's key role as a viral protein processing protease in other coronaviruses (SARS-CoV, MERS-CoV) and influenza viruses, this new class of inhibitors may be effectively utilized as a broad-spectrum antiviral.

Acknowledgements

Chapter 3, in part, is a reprint of the material as it appears in A novel class of TMPRSS2 inhibitors potently block SARS-CoV-2 and MERS-CoV viral entry and protect human epithelial lung cells. Mahoney, Matthew, Damalanka, Vishnu C., Tartell, Michael A., Chung, Dong H., Lourenço, André L., Pwee, Dustin, Bridwell, Anne E.M., Hoffmann, Markus, Voss, Jorine, Karmakar, Partha, Klingler, Andrea M., Thompson, Cassandra E., Lee, Melody, Klampfer, Lidija, Stallings, Christina L., Rothenberg, Marc E., Whelan, Sean P.J., O'Donoghue, Anthony J., Craik, Charles S., Janetka, James W., Proceedings of the National Academy of Sciences, 2021. The thesis author was a co-author of this paper.

CHAPTER 4

The COVID-19 pandemic has had a devastating effect on both global health and the functioning of society, and prophylactic and therapeutic intervention strategies are urgently needed. Currently, there has been an intense global effort directed towards the development of an effective COVID-19 vaccine, with several candidates, including two mRNA vaccines and a chimpanzee adenovirus-vectored vaccine, completing phase III human clinical trials and now in widespread use globally. In addition to an effective prophylactic vaccine, the control of COVID-19, and potentially future SARS coronavirus zoonoses, also requires efficacious antiviral therapeutics, particularly considering the rapid emergence of variant strains.

While antiviral drug discovery for SARS-CoV-2 has been the subject of significant effort, most molecules currently in clinical trials are repurposed from other indications for which they were originally approved. Remdesivir is currently the only antiviral drug to be approved by the U.S Food and Drug Administration for the treatment of COVID-19. Whilst this molecule has been reported to show some efficacy during early infection, the drug has performed poorly in several trials where it was deemed ineffective, including a recent report from the World Health Organization that suggested remdesivir provided little to no effect in the outcome of COVID-19 infections in hospitalized patients. At the present time, one of the most effective means of improving COVID-19 patient outcomes has been the use of glucocorticoid dexamethasone which serves to reduce inflammation-mediated lung injury. Taken together, despite significant effort from the global research community, there is still an urgent need to discover effective antivirals for COVID-19 infection that operate through novel mechanisms of action and that are distinctive to the molecules currently in use. While there are obvious benefits to post-exposure drug

therapies, the development of a pre-exposure prophylaxis approach, such as what has been employed for HIV, would also be transformative for protecting vulnerable communities.

Recognition and entry of SARS-CoV-2 into target cells relies on binding between the receptor-binding domain of an envelope homotrimeric spike glycoprotein and the host cellular receptor, angiotensin-converting enzyme 2. Recently, a second receptor protein, a transmembrane glycoprotein of the immunoglobulin superfamily, known as CD147, has been identified as mediating spike protein interaction and viral uptake via endocytosis. Each monomeric unit of the spike protein contains an S1 and S2 subunit that mediate attachment and membrane fusion with host cells, respectively. Host cell entry requires priming of the spike protein by cleavage at the S1/S2 and the S2′ site that enables fusion of viral and cellular membranes. This cleavage has been shown to be carried out primarily by the membrane-bound serine protease TMPRSS2, but can also be performed by the cysteine protease, cathepsin L. Following entry of the virus into the cell via an endosomal pathway, CatL is responsible for S1 cleavage at acidic pH, conditions where TMPRSS2 is not catalytically functional. Overexpression of CatL in human cell lines enhances SARS-CoV-2 spike-mediated viral entry, while circulating CatL is elevated during COVID-19 disease and correlates with progression and severity. Finally, it is known that expression of CatL, but not cathepsin B is up-regulated by interleukin-6. This is of importance, as there is early evidence that Interleukin-6 is a surrogate inflammatory marker for severe COVID-19 disease with poor prognosis. This would imply that CatL is upregulated under these conditions and would therefore be a potentially important target for controlling excessive pathology.

This dual role of CatL in the establishment and progression of COVID-19 pathology has therefore reinforced the enzyme as a key drug target for SARS-CoV-2. The importance of both

TMPRSS2 and CatL for facilitating viral entry and replication is highlighted by the effectiveness of TMPRSS2 inhibitors, camostat mesylate and nafamostat mesylate and the pan-cysteine protease inhibitors E64 and K777 to reduce virus infection levels of SARS-CoV-2 (and SARS-CoV) in a range of human cell lines. Following uncoating and release of the viral RNA from the endosome, translation of the two large viral reading frames gives rise to the polyproteins pp1a and pp1ab that are subsequently processed by two viral proteases: the main protease (Mpro) and the papain-like protease (PLpro). This gives rise to several non-structural proteins that subsequently orchestrate viral replication and release from infected cells, to infect new cells. As such, both Mpro and PLpro are also promising antiviral targets for SARS-CoV-2. Gallinamide A 1 (also known as symplostatin 4) is a modified depsipeptide natural product that was independently discovered from marine cyanobacteria of the Schizothrix genus in Panama and Symploca in Florida. The natural product has several unusual structural features including a pyrrolinone derived from l-alanine and an α,β-unsaturated imide moiety. Notably, gallinamide A has been demonstrated to be a potent covalent inhibitor of several parasite-derived cysteine proteases, as well as human CatL, with several synthetic analogues of the natural product also shown to have potent in vivo antimalarial activity in a murine model. Given the importance of CatL for cellular entry of SARS-CoV-2, we sought to investigate whether the CatL inhibitory activity of gallinamide A could be leveraged for SARS-CoV-2 antiviral activity. Towards this end, in May 2020 we assembled an international consortium to investigate gallinamide A, together with 32 synthetic natural product analogues, as novel inhibitors of SARS-CoV-2 entry. We report herein that several analogues exhibit potent inhibitory activity against CatL with IC50 values in the low nanomolar to picomolar range. Several of these gallinamide A-inspired molecules also possess selectivity over Cathepsin B and other related cathepsin proteases and do

not inhibit the two viral proteases Mpro and PLpro, or host cell proteases furin and TMPRSS2. We demonstrate here the potential of cathepsin L as a COVID-19 antiviral drug target.

Materials and Methods

1. Protease screening of gallinamide A (1) and analogues 2-33.

Active recombinant human TMPRSS2 was purchased from Cusabio Technology and assayed at a final concentration of 3 nM in 25 mM Tris-HCl, 150 mM NaCl, 5 mM Cacl2, 0.01% Triton X-100, pH 8.0, with 86 μM Boc-QAR-AMC. Recombinant human furin was purchased from R&D Systems and assayed in 25 mM Tris-HCl, 150 mM NaCl, 5 mM CaCl2, 0.01% Triton X-100, pH 8.0 with 50 μM pERTKR-AMC at a final concentration of 1.9 nM. TMPRSS2 and furin were pre-incubated with 100 μM of gallinamide A and analogues for 30 minutes. The reaction was initiated with the addition of the substrate. DMSO was used as a vehicle control. All assays were completed at room temperature with a final volume of 30 μL in triplicate wells on a black 384-well plate. Fluorescence was measured at 360/460 nm excitation/emission using a Biotek HTX plate reader. Activity was normalized to wells lacking inhibitor but containing 0.01% DMSO in assay buffer.

Results

Recent studies have shown that peptide inhibitors of CatL and other related cysteine proteases also possess inhibitory activity against SARS-CoV-2 Mpro. To assess the comparative activity of gallinamide A against human CatL and the viral proteases Mpro and PLpro, we incubated these proteases with 10 μM of the natural product, and quantified the remaining activity using fluorogenic substrates. CatL activity was completely inhibited by

gallinamide A at this concentration, while no inhibition of Mpro or PLpro was observed. We also confirmed the gallinamide A did not inhibit the activity of two key host proteases involved in SARS-CoV-2 entry into cells, namely furin and TMPRSS2, up to a concentration of 50 µM (Figure 4.1).

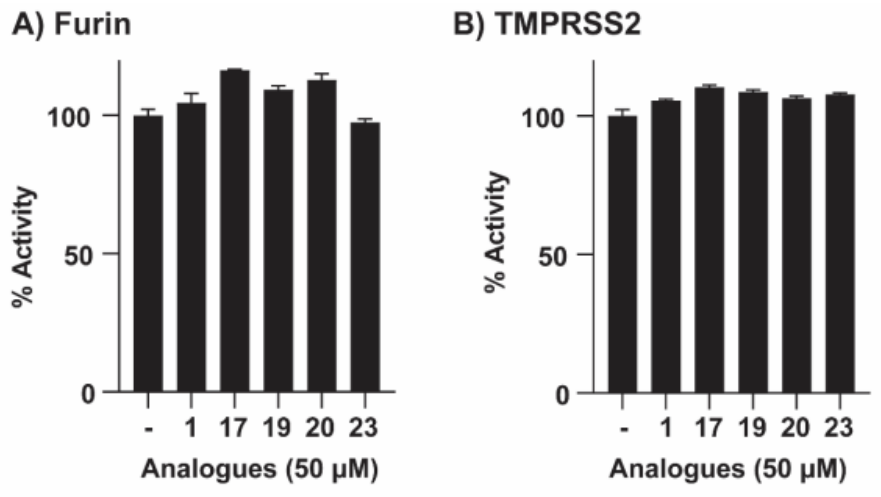

Figure 4.1: Gallinamide A and analogues do not inhibit furin or TMPRSS2.

Discussion

Cathepsin L is a lysosomal enzyme that plays a key role in intracellular protein degradation in our cells. Expression of this enzyme is dysregulated in several human diseases, including cancer, arthritis, and diabetic nephropathy, with therapeutics in development for these ailments. Mice deficient for this gene exhibit hair loss, bone and heart defects, and enhanced susceptibility to bacterial infection. Therefore, targeting of this host enzyme for treatment of SARS-CoV-2 infections may pose a risk for side-effects. However, treatment for coronavirus infection would likely be short-term, aiming to reduce viral entry and early replication until host innate and adaptive responses can be developed.

We demonstrate here that the marine natural product, gallinamide A and several synthetic analogues, are potent inhibitors of CatL, a key host cysteine protease involved in the pathogenesis of SARS-CoV-2. Lead molecules possessed selectivity over CatB and other related human cathepsins or proteases used for SARS-CoV-2 entry, furin, and TMPRSS2.

Acknowledgements

Chapter 4, in part, is a reprint of the material as it appears in Potent Anti-SARS-CoV-2 Activity by the Natural Product Gallinamide A and Analogues via Inhibition of Cathepsin L. Ashhurst, Anneliese S., Tang, Arthur H., Fajtová, Pavla, Yoon, Michael C., Aggarwal, Anupriya, Bedding, Max J., Stoye, Alexander, Pwee, Dustin, Drelich, Aleksandra, Li, Linfeng, Meek, Thomas D., McKerrow, James H., Tseng, Chien-Te, Larance, Mark, Turville, Stuart, Gerwick, William H., O'Donoghue, Anthony J., Payne, Richard J., Journal of Medicinal Chemistry, 2022. The thesis author was a co-author of this paper.

REFERENCES

1. Kisselev AF, Goldberg AL. Proteasome inhibitors: from research tools to drug candidates. *Chem Biol.* 2001;8(8):739-758. doi:10.1016/s1074-5521(01)00056-4.

2. Goldberg AL. Development of proteasome inhibitors as research tools and cancer drugs. *J Cell Biol.* 2012;199(4):583-588. doi:10.1083/jcb.201210077.

3. Nelson RK, Bush A, Stokes J, Nair P, Akuthota P. Eosinophilic Asthma. *J Allergy Clin Immunol Pract.* 2020;8(2):465-473. doi:10.1016/j.jaip.2019.11.024.

4. O'Donoghue AJ, Jin Y, Knudsen GM, Perera NC, Jenne DE, Murphy JE, Craik CS, Hermiston TW. Global substrate profiling of proteases in human neutrophil extracellular traps reveals consensus motif predominantly contributed by elastase. *PLoS One*. 2013;8(9):e75141. Published 2013 Sep 20. doi:10.1371/journal.pone.0075141.

5. Mahoney M, Damalanka VC, Tartell MA, Chung D, Lourenço AL, Pwee D, Mayer Bridwell AE, Hoffmann M, Voss J, Karmakar P, Azouz NP, Klingler AM, Rothlauf PW, Thompson CE, Lee M, Klampfer L, Stallings CL, Rothenberg ME, Pöhlmann S, Whelan SPJ, O'Donoghue AJ, Craik CS, Janetka JW. A novel class of TMPRSS2 inhibitors potently block SARS-CoV-2 and MERS-CoV viral entry and protect human epithelial lung cells. Proc Natl Acad Sci U S A. 2021;118(43):e2108728118. doi:10.1073/pnas.2108728118.

6. Ashhurst AS, Tang AH, Fajtová P, Yoon MC, Aggarwal A, Bedding MJ, Stoye A, Beretta L, Pwee D, Drelich A, Skinner D, Li L, Meek TD, McKerrow JH, Hook V, Tseng CT, Larance M, Turville S, Gerwick WH, O'Donoghue AJ, Payne RJ. Potent Anti-SARS-CoV-2 Activity by the Natural Product Gallinamide A and Analogues via Inhibition of Cathepsin L. J Med Chem. 2022;65(4):2956-2970. doi:10.1021/acs.jmedchem.1c01494.